J - Resistance curve of X60 steel using SE(T) specimens by elastic compliance and potential drop methods

André LM Carvalho[1*], Juliana P Martins[2], Roberto R. Piovatto[3] and Waldek W Bose Filho[3]

[1] Department of Materials Engineering, Ponta Grossa State University, 84030-900, PR, Brazil

[2] Chemical Engineering, UTFPR, 84016-210, Ponta Grossa, PR, Brazil

[3] Department of Materials, Aeronautics and Automotive Engineering, EESC-USP, 13566-590, São Carlos, SP, Brazil

[*] 'andrelmc@uepg.br

Keywords: J-R curve, SE(T) specimen, unloading compliance, potential drop, API 5L X60 steel

Abstract. In this article investigate J-R curves behavior through standard single-specimen technique using both the unloading compliance and potential drop method for measuring crack extension performed in shallow and deep cracked nonstandard specimens. Analysis from Electron Backscattered Diffraction (EBSD) was performed in the fracture regions where took place the delamination phenomena to obtain crystallography orientation all cleavage fracture zone. The results show in the delamination where predominates cleavage fracture has displayed crystallography orientation of $\{3\ 3\ 5\} < \bar{5}\bar{5}6 >$ with maxim intensity of 3.715. Potential drop method has showed the best performed in predict initiate crack length in comparison to unloading compliance.

Introduction

Large–diameter, high-pressure gas transmission pipelines have been used more and more widely all over the world. With the development of the pipeline network, safety and maintenance become an important task. The accurate prediction of fracture for oil and gas pipelines with crack-like flaws is essential for fitness-for-service (FFS) methodology, for instance, repair decisions and life-extension procedures and to ensure fail-safe operations which avoid costly leaks and rupture. As defects of various sizes are detected and thinning of pipe walls by aggressive gas gradients is inevitable with time, a better understanding of the fracture toughness and cracking resistance of the pipe materials is required [1]. Structural pipeline steels generally exhibit a significant increase in fracture toughness, characterized by the *J-integral*, over the first few millimeters of stable crack extension [2]. The *J-integral* values have been used extensively as indexes of material toughness for alloy design, material processing, material selection and specification, as well as quality assurance [3]. The fracture toughness J_{IC} and *J-integral* resistance curves, namely, *J-R* curves have been also used in the integrity assessment of engineering structures with ductile crack tearing or growth. High pipeline steel press, it shows low-constraint because thin wall structure did not supply the strain plane stress. Whereas, the fracture toughness test standard ASTM E1820 was developed only for high constraint specimens, like deep cracked single-edge notched bend SE(B) and compact tension C(T) specimens with the expectation that the results represent lower bound toughness. Accordingly, the application of fracture toughness from high-constraint specimens to low-constraint geometries introduces a degree of conservatism into design [4]. While most of nonstandard specimens (SE(T) or real cracked structures (pipelines) have low crack-tip constraint. As results, the test data of J_{IC} and *J-R* curves are strongly depend on the crack size or crack-tip constraint level [5]. Application of the measured fracture toughness to real structures pipeline steels is thus resisted with the justification that the real structure has only shallow cracks and the ASTM fracture toughness measures do not apply [6]. As a consequence, the determination of J-R curves for both deep and shallow cracked nonstandard specimens SE(T) becomes very important. Furthermore, the steel has shown banding as observed in hot rolled plate and characterized by microstructure of alternate layers of ferrite and pearlite. This feature contributes to appearance of delamination phenomena during the fracture toughness testing. This manner, the present work aims to investigate evaluation of *J-R* curves from standard single-specimen technique using both the unloading compliance and potential drop method for measuring crack extension performed in shallow and deep cracked nonstandard specimens. In the work also the plastic component of J integral was obtained from of crack mouth open displacement (CMOD) data. Analysis from Electron Backscattered Diffraction (EBSD) was performed in the fracture regions where took place the delamination phenomena to obtain crystallography orientation all cleavage fracture zone.

Experimental Procedure

The material considered in this investigation was an API 5L-X60 steel, used in oil and gas pipeline. The mechanical tensile test from standard cylindrical was carried out at room temperature following ASTM E8M standard requirements. The experimental results of the mechanical properties from tensile tests were: elastic modulus 207 GPa, 0.2 yield stress 499 MPa, ultimate tensile strength 625 MPa and elongation 21% in the longitudinal (L) direction. Results obtained are in accordance with the requirements prescribed by (API, 2000), this standard defines minimum values for yield strength and ultimate strength of, 448 MPa (65,000 psi) and 552 MPa (80,000 psi) for this steel grade. The chemical composition of this material is presented in Table 1.

Table 1. Chemical composition of API 5L-X60 steel (mass. %)

Element	C	Mn	Si	P	S	Cr	Ni	V	Ti	Nb	Al
% weight	0,098	1,63	0,33	0,02	0,02	0,01	0,02	< 0,010	0,022	0,04	0,051

EBSD scans were performed a Zeiss EVO MA10 model scanning electron microscope equipped with TSL 5.2 OIM data collector/ analyzer software. The scan area was performed along all perpendicular surface at the fracture surface where took place the delamination in which predominates the cleavage fracture. This area consist the microstructure of alternate layers of ferrite and pearlite.

Specimens Geometry

The single edge notched tensions SE(T) specimens were used to measure *J-R* curves. All specimens crack planes were oriented in the TL orientation by ASTM E399. Schematic drawing of this specimen is shown in Fig. 1. The SE(T) specimen has following dimensions: length of reduction section of 156 mm, radius of fillet of 10 mm, overall length of 276 mm, width, W, of 32 mm and thickness of 12.5 mm. This specimen was loaded with a centered pin at center distance of 214 mm. Crack length to width ratios (a/W) of 0.21 and 0.52 were investigated, corresponding shallow and deep cracks respectively. The specimens were loaded in three-point bending with a span of 128 mm, after precracking by fatigue according to the procedure in ASTM E1820-05. Specimens were side grooved using a Charpy cutter to a total thickness reduction of 20%, in an attempt to develop plane strains conditions along crack front. All specimens were tested at room temperature.

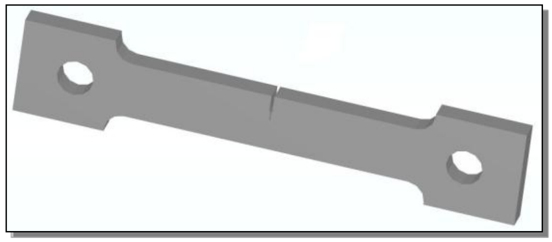

Figure 1. Schematic drawing of specimens SE(T) under study.

Test Technique and J-R Curves Determination

In this investigation the J-R curves of X60 pipeline steel were performed by both unloading compliance (UC) and constant current potential drop methods (PD), these tests procedure were carried out which allowed monitoring the specimens crack length using a single specimen technique. After test, the specimens were heat tinted and then broken in liquid nitrogen. The initial and final crack lengths were measured on the fracture surface by the 9-point technique as described in ASTM E1820. For the SE(T) specimens a standard clip gage was installed to measure the crack mouth opening displacement, CMOD, which was used for crack length estimation. Current estimation procedures (which form the basis of ASTM E1820 standard) employ load line displacement (LLD) records to measure fracture toughness resistance data incorporating a crack growth correction for J. In the present work an alternative method which will be to use from crack mouth opening displacement (CMOD) to determine the plastic component of J integral. As the SE(T) specimens, a standardized procedure to calculate the J-resistance is not available, k, η, γ factors used in the Eqs. 1 up 6 for the required elastic and plastic component of the *J* integral were taken from [7,8]. As also, two rotation corrections were needed, one to correct the COD to obtain the corrected compliance, before of the estimated crack length for the partial unloading. Second correction, was also used to apply a rotation correction to the load line compliance, before calculating the elastic and plastic area components used (Eqs. 1 and 2) to calculate J components. Both procedures were taken from [9] and were used in according ASTM E1152.

J integral Analysis

The *J* integral was calculated by separating it into elastic and plastic components and calculating the components separately. The elastic J component, J_{el}, is calculated from

$$J_{el} = \frac{k^2}{E'} \tag{1}$$

$$K_{(i)} = \sqrt{\pi a} \times \frac{P}{WB} \times f\left({a_i}/{W} \right) \tag{2}$$

where a/W is polynomial function:

$$f\left({a_i}/{W} \right) = \begin{bmatrix} -0{,}0917 + 22{,}392 \times (a/W) - 141{,}96 \times (a/W)^2 + 449{,}72 \times (a/W)^3 \\ -645{,}59 \times (a/W)^4 + 363{,}52 \times (a/W)^5 \end{bmatrix} \tag{3}$$

where K is the elastic stress intensity factor for the specimen, $E' = E/(1-\upsilon^2)$, and E and υ are the elastic modulus and Poisson's ratio, respectively. The plastic component J, J_{pl}, is calculated using the ASTM Standard E1152 equation:

$$J_{pl} = J_{pl(i-1)} + \frac{\eta_i}{b_i}\left[\frac{A_{pl(i)} - A_{pl(i-1)}}{B_N}\right]\left[1 - \frac{\gamma_i (a_i - a_{(i-1)})}{b_i}\right] \tag{4}$$

A_{pli} = area under the load versus plastic load line displacement curve to increment i,
η_i = the plastic η factor at crack length a_i
b_i = the incremental remaining ligament
W = the specimen width and

$$\eta_i^{CMOD} = 0{,}9167 + 0{,}0837\left(a/W\right) \tag{5}$$

$$\gamma_i^{CMOD} = -0{,}0833 + 0{,}0837\left(a/W\right) + \left(\frac{-0{,}0837 + 0{,}0837\left(a/W\right)}{0{,}9167 + 0{,}0837\left(a/W\right)}\right) \tag{6}$$

Formulas for the compliance relationships, K's and η's, γ's used to obtain the J-R curves for the SE(T) specimen are in according [7,8], respectively.

Crack Extension Measurements

The fracture toughness test standard ASTM E 1820-05 is designed for the *J* determination using the unloading compliance method to standard specimens for crack extension measure. However, the SE(T) specimens are categorized as nonstandard one, to which the E1820 may not be applicable. For this reason, it is necessary to apply in the elastic compliance method an adjustment compliance equation to obtain measure crack length or incremental crack to the SE(T) specimens. In the present study, compliance equation to the SE(T) specimens used is according [8], developed compliance equation used to the SE(T) specimens (pin-loaded) with initial crack length *a* varied producing various ratios of *a*/W 0.1 to 0.7. Other method for crack extension measure used in the work was constant current potential drop. The Eq. 9 was resulted of normalized voltage V= (V_i –V_0)/V_0 versus normalized crack depth a/W, where V_0 is reference value measured at the start of the test, V_i is instantaneous voltage during crack growing as following:

$$a/W = 1.0056 - 2.8744u' + 5.4420u'^2 - 12.510u'^3 + 16.102u'^4 - 7.0642u'^5 \tag{7}$$

$$u' = \frac{1}{1 + \sqrt{\frac{E' B_e \delta}{P}}} \tag{8}$$

$$a_i / W = 0{,}01668 + 0{,}19989\left(V_i / V_0\right) - 0{,}01176\left(V_i / V_0\right)^2 \tag{9}$$

For side-grooved specimens, the thickness *B* is replaced by B_e namely, $B_e = B - (B - B_N)^2 / B$, where B_N is the net specimen thickness at the side groove roots.

Results and Discussion

Results from fractographic investigation of fracture toughness test pieces were observed the presence of single and multiple delamination cavities (splits) as can be drawn in Fig. 2 a) e 2b). The fracture surface profile is predominantly flat along the whole ligament length on a macroscopic point of view as shown by Fig. 2 a) and b). Beside the delamination, a classical profile with dimples was observed in the SEM. Therefore, the phenomenon responsible for crack initiation and growth is void growth and coalescence internal to the specimens. In this API 5L steel, delamination is believed to occur due to decohesion of ferrite-pearlite interface [10]. As the out-of-plane constraint is highest at the centre of the specimen, the delamination in the middle part of all are most severe. Reported experimental data by [1] indicated large delaminations start from the initial crack front and growth with crack extension to the final fracture point. The same characteristic occurred here, as can be displayed in Fig. 2 a) and b). Secondary delaminations are concentrated at the 1/4 thickness points from the free surfaces and similar to the main delamination (Fig. 2 b). The main delamination at the centre of specimen releases the out-of-plane constraint completely on the middle plane [2].

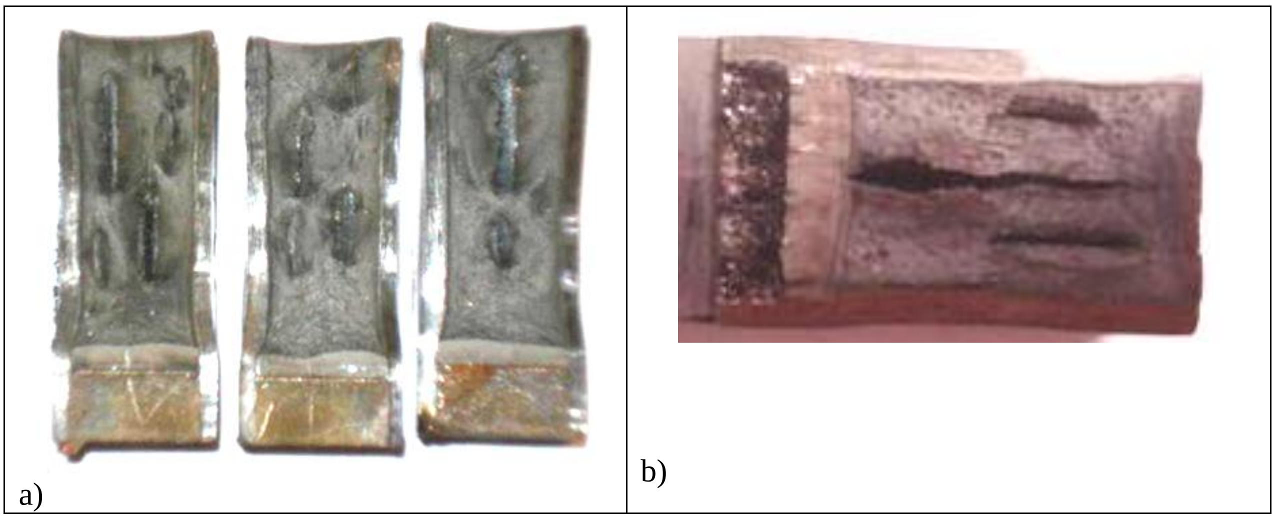

a) b)

Figure 2. a) Typical fracture surface of SE(T) specimens with multiple delaminations, b) fracture surface of the SE(T) specimen with main and secondary delaminations.

Concerning the delamination phenomena was performed analyses by EBSD technique in the fracture regions where took place the delamination to obtain crystallography orientation all cleavage fracture zone. This manner in Fig. 3 shows the orientation image mapping along all perpendicular surfaces at the fracture surface where took place the delamination where indicated a grain size average of 4.7 μm. It is possible to notice in the Figs. 4, a predominance {111} plane which correspond the ferrite while {001} plane is associated to cementite. In relation to Fig. 5 can be seen a preferential orientation of $\{3\ 3\ 5\} < \bar{5}\bar{5}6 >$ with maxim intensity of 3.715. Figs. 6 and 7 display the experimental crack growth resistance curve from Eqs. 1- 9, for the shallow and deep specimens, the measured crack length values were used from both unloading compliance and potential drop method. It is possible to notice in Figs. 6 and 7, the features of ductile tearing behavior along crack growth resistance curve for both crack length to width ratios (a/W) of 0.21 and 0.52, as also, an elevated fracture toughness behavior for first condition in comparison with the deep-cracked specimens (Fig.7). Both features are observed at crack initiation and throughout the ductile crak growth region. Such behavior is entirely consitent with previous results obtained by [4,7]. In relation to predict and measured crack length value to initiate and final for both methods, in the shallow cracked specimens the potential drop has obtained a difference of 9.6% and 26% while unloading compliance was 16% and -2.54% , respectively.

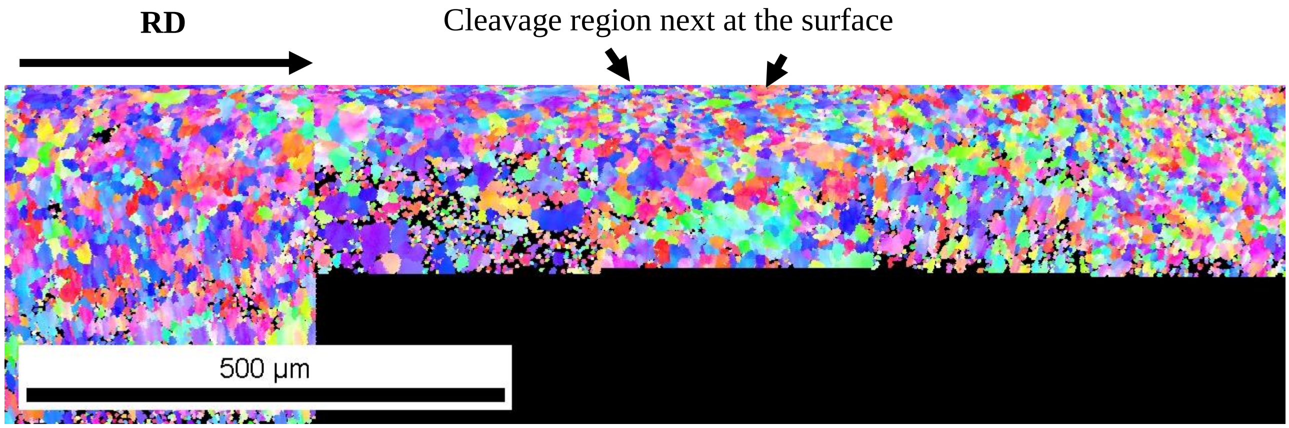

Figure 3. Orientation image mapping (OIM), from EBSD data along all perpendicular surface of fracture surface in the delamination region that involve cleavage region.

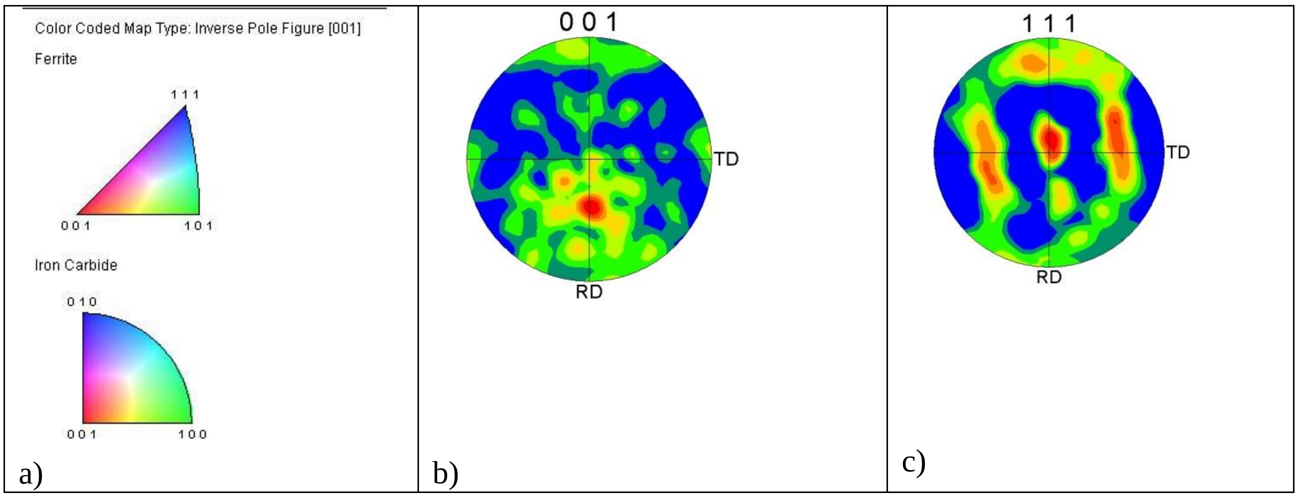

Figure 4. a) Inverse pole figure of ferrite and cementite; b) PF 001 of cementite with symmetry triclinic; c) PF 111 of ferrite with triclinic symmetry.

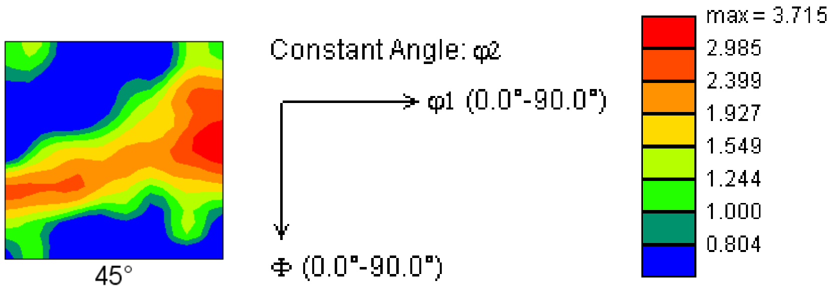

Figure 5. Orientation distribution function (ODF) $\varphi_2 = 45°$ revealing presence of $\{3\ 3\ 5\} < \bar{5}\bar{5}6 >$ component, which appears with maxim intensity of 3.715.

Whereas the deep cracked specimens both methods have resulted equivalent, corresponding a difference between the predicted a measured of 0.41% and 1.14%, respectively.

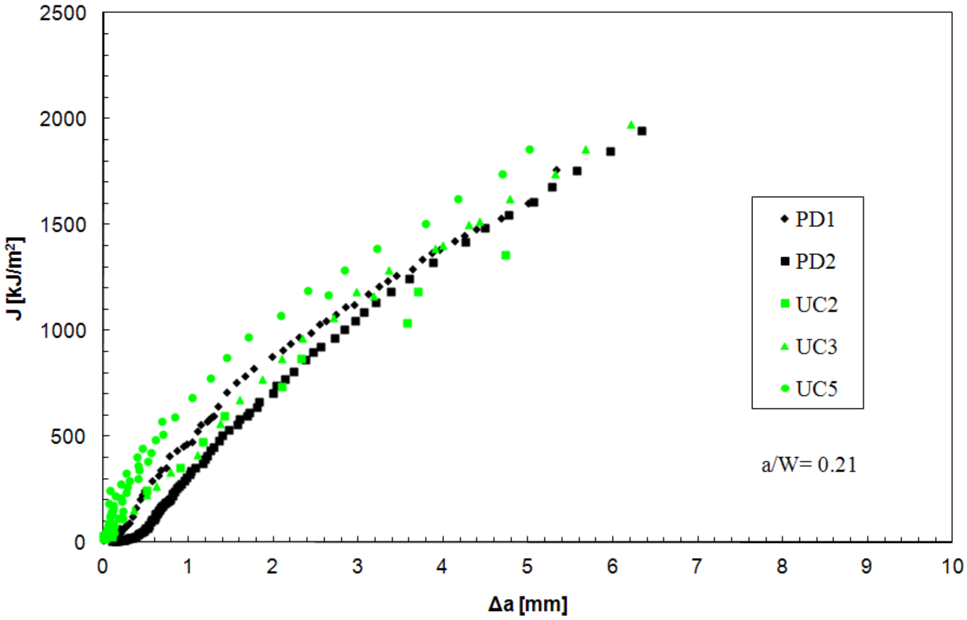

Figure 6. Typical load versus crack extension curves for SE(T) specimens for shallow crack a/W= 0.21.

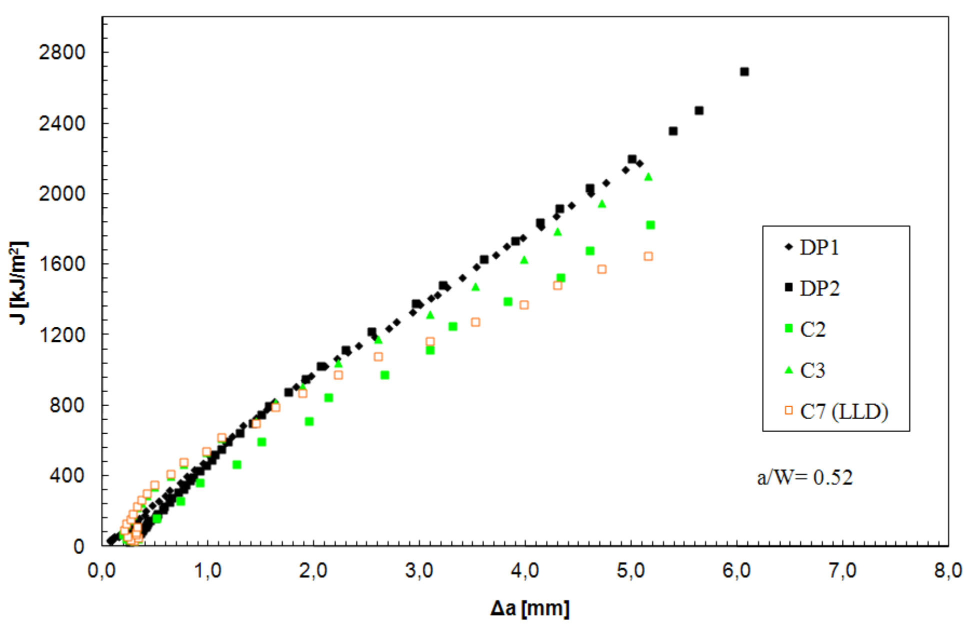

Figure 7. Typical load versus crack extension curves for SE(T) specimens for deep crack a/W= 0.52.

Concluding Remarks

The present work investigated evaluation of *J-R* curves in SE(T) specimens of X60 steel from standard single-specimen technique using both the unloading compliance and potential drop methods for measuring crack extension performed in shallow and deep cracked nonstandard specimens. The plastic component of J integral was obtained from of crack mouth open displacement (CMOD) data. Analysis by EBSD technique was performed in the fracture regions where took place the delamination phenomena to obtain crystallography orientation all cleavage fracture zone. The results obtained can be summarized as follows: It was observed single and multiple delaminations (split) at fracture surface from the shallow and deep cracked specimens. This suggest, the delamination decreases the constraint, thus increasing the compliance of the specimens, accordingly, it can affects the fracture toughness values along of resistance curve. In the delamination where predominates cleavage fracture has displayed crystallography orientation of {3 3 5} $< \bar{5}\bar{5}6 >$ with maxim intensity of 3.715. In relation to predict and measured crack length value, it was evidenced greater difficulty for both method for measuring crack extension in shallow cracked specimens. Potential drop method has showed the best performed in predict initiate crack length in comparison to unloading compliance. While final crack length value the unloading compliance has obtained lower difference relation to measured crack length value. On the other hand, for the deep cracked condition, both methods have shown to is very agreement with the measured value.

5. Acknowledgements

This work is supported by the Fundação de Amparo à Pesquisa do Estado de São Paulo (FAPESP) through Grant 04/02856-0, as also by the Ministry of Science and Technology of Brazil under a Postdoctoral Fellowship (BPD/CAPES/PNPD/Process N° 23038.008242/2010–08). Authors also acknowledge the Brazilian State Oil Company (Petrobrás) for making available the SE(T) fracture specimens used in testing of the API 5L X60 pipeline plate.

References

[1] W. Guo, H. Dong, M. Luand X. Zhao: Int. J. Press. Vessel. Pip., V. 79 (2002), p. 403.
[2] E.Jr Hippert and C. Ruggieri (Proc. Press. Vessel. Pip. Conf., ASME,Atlanta, GA, US 2001).
[3] X.K.Shu, and S.K. Jang, Engng. Fract. Mech., Vol. 68 (2001), p. 285.
[4] Shu, X.K. and Leis, B.N., 2005, Proc. Press. Vessel. Pip. ASME, Denver, Colorado, USA.
[5] T. V. Pavankumar, J. Chattopadhyay, H.S.Dutta, and H.S. Kushwaha, Int. J. Press. Vessel. Pip. Vol.79(2002), p. 127.
[6] X.K. Zhu and J.A Joyce,: Engng. Fract. Mech. Vol. 74 (2007), p. 2261.
[7] J.A. Joyce, E.M Hackett and C.Roe in: *Constraint Effects in Fracture*, ASTM STP (Special Technical Publication) edited by E.M.Hackett, K.-H.Schwalbe and R.H.Dodds, American Society of Testing and Materials, Philadelphia, (1993) in press.
[8] S. Cravero, and C. Ruggieri: Engng Fract. Mech. Vol. 74 (2007) p.2735.
[9] J.A. Joyce and R.E. Link, in: *Effects of Constraint on Upper-Shelf Fracture Toughness*, edited by W.G.Reuter, J.H.Underwood and J.C.Jr. Newman Vol. 26, American Society for Testing and Materials, Philadelphia, (1995) in press.
[10] P. Shanmugan and S.D. Pathak: Engng. Fract. Mech. Vol.53 (1996), p. 991.